NEOPLASIA
www.neoplasia.com

Volume 31 Number xxx Month 2022 pp. 100815

Original Research

Suppression of tumor progression by thioredoxin-interacting protein-dependent adenosine 2B receptor degradation in a PLAG-treated Lewis lung carcinoma-1 model of non–small cell lung cancer

Guen Tae Kim [a]; Eun Young Kim [a]; Su-Hyun Shin [a]; Hyowon Lee [a]; Se Hee Lee [a]; Ki-Young Sohn [a]; Jae Wha Kim [b,*]

[a] Enzychem Lifesciences, 10F aT Center 27 Gangnam-daero, Seoul, South Korea
[b] Korea Research Institute of Bioscience and Biotechnology (KRIBB), 125 Kwahak-ro, Daejeon, South Korea

Abstract

Extracellular adenosine in the tumor microenvironment plays a vital role in cancer development. Specifically, activation of adenosine receptors affects tumor cell growth and adenosine release.

We examined the anti-tumor efficacy of 1-palmitoyl-2-linoleoyl-3-acetyl-rac-glycerol (PLAG) in animal models, revealing the role of PLAG in inhibiting tumor progression by promoting the degradation of adenosine 2B receptors (A2BRs) in tumors. PLAG induced the expression of thioredoxin-interacting protein (TXNIP), a type of α-arrestin that accelerates A2BR internalization by interacting with A2BR complexes containing β-arrestin. Engulfed receptors bound to TXNIP were rapidly degraded after E3 ligase recruitment and ubiquitination, resulting in early termination of intracellular signals that promote tumor overgrowth. However, in control cancer cells, A2BRs bound to protein phosphatase 2A and were returned to the cell membrane instead of being degraded, resulting in continuous receptor-mediated signaling by pathways including the Raf-Erk axis, which promotes tumor proliferation. A TXNIP-silenced cell-implanted mouse model and TXNIP knockout (KO) mice were used to verify that PLAG-mediated suppression of tumor progression is dependent on TXNIP expression. Increased tumor growth was observed in TXNIP-silenced cell-implanted mice, and the anti-tumor effects of PLAG, including delayed tumor overgrowth, were greatly reduced. However, the anti-tumor effects of PLAG were observed in cancer cell-implanted TXNIP-KO mice, which indicates that PLAG produces anti-tumor effects by enhancing TXNIP expression in tumor cells.

These essential functions of PLAG, including delaying tumor growth via A2BR degradation, suggest innovative directions for anticancer drug development.

Neoplasia (2022) 31, 100815

Keywords: 1-Palmitoyl-2-linoleoyl-3-acetyl-rac-glycerol (PLAG), Thioredoxin-interacting protein, Adenosine 2B receptors, Degradation, Signal termination

Abbreviation: PLAG, 1-Palmitoyl-2-limoleoyl-3-acetyl-roc-glycerol; A2BR, Adenosine 2B Receptor; TXNIP, Thioredoxin interacting protein; NEDD-4, Neural precursor cell-expressed developmentally downregulated protein 4; PP2A, Phosphatase 2A; KO, Knock-out; eAdo, extracellular Adenosine; GPCR, G-protein coupled receptors; MAPK, Mitogen-activated protein kinase; LLC-1, Lewis Lung Carcinoma; MOA, Mechanism of Action; TME, Tumor microenvironment; EGFR, Epidermal growth factor receptor; RTK, Receptor tyrosine kinase.

* Corresponding author.
E-mail address: wjkim@kribb.re.kr (J.W. Kim).

Received 17 May 2022; received in revised form 23 May 2022; accepted 8 June 2022

https://doi.org/10.1016/j.neo.2022.100815

Introduction

Extracellular adenosine, which is mainly secreted by tumor tissue, stimulates tumor cell proliferation and regulates the immune response, which is advantageous for tumor development [1–3]. In particular, the cell signaling pathways activated through the adenosine receptor family induce both overactivation of cancer cells and inhibition of the anticancer immune response. A recent study found that extracellular adenosine stimulates adenosine 2B receptor (A2BR), which induces tumor growth, promotes metastasis, and effectively induces the tumor microenvironment (TME). Induction of A2BR activity by extracellular adenosine activates tumor growth–related signaling pathways, such as the Erk pathway, and induces cAMP accumulation. In addition, antigen-presenting cells, which express A2BRs, in the TME promote tumor hyperactivity through inhibition of cytotoxic T-cell activity [4–9]. In previous studies, the specific inhibition of A2BRs effectively inhibited tumor overgrowth in multiple tumor models [10–12]. Therefore, the inhibition of A2BRs in tumors has become an important topic of cancer research.

A2BR is a type of G protein–coupled receptor (GPCR) that is activated when it binds to extracellular adenosine. Ligand-binding receptors initiate intracellular trafficking, and endocytosis of GPCRs occurs during the receptor desensitization process [13–15]. Recent studies have shown that intracellular signaling by ligand-specific receptors is induced during intracellular trafficking [16–18]. Endocytosis and intracellular GPCR signaling rely primarily on assembled complexes, such as those containing arrestins. GPCRs in endosomes activate signaling pathways, such as the mitogen-activated protein kinase (MAPK) pathway and contribute to tumor cell proliferation [19–21]. Whether an internalized GPCR is degraded or returns to the cell membrane is determined by the assembly of a receptor–protein complex [22–25].

Thioredoxin-interacting protein (TXNIP), a member of the α-arrestin family, is an important scaffold protein that induces endocytosis of receptors and transport proteins [26,27]. α-Arrestin, which contains PPxY motifs, recruits E3 ligases and induces receptor ubiquitination and degradation to quickly and effectively terminate intracellular signaling [28–30]. Rapid adenosine receptor internalization and degradation are optimal processes for terminating intracellular signaling initiated by adenosine receptor activation, preventing excessive and continuous receptor activation.

1-Palmitoyl-2-linoleoyl-3-acetyl-rac-glycerol (PLAG) is present in the antlers of sika deer and can be synthesized from glycerol, palmitic acid, and linoleic acid. Previous studies have shown that PLAG can effectively alleviate symptoms of severe inflammatory diseases, such as acute lung injury, oral mucositis caused by chemoradiotherapy, and gout [31–34]. In addition, the abnormal metastasis of A549 non–small cell lung cancer cells and the excessive growth of the triple-negative breast cancer cell line MDA-MB-231 were also effectively inhibited by PLAG [35,36]. Based on these results, we investigated the inhibitory effect of PLAG on tumor progression in Lewis lung carcinoma (LLC1) cell-implanted mouse models. PLAG treatment effectively controlled tumor progression by inducing TXNIP expression. TXNIP is associated with the rapid internalization and degradation of A2BRs, resulting in early termination of receptor-mediated signaling pathways that promote tumor proliferation, including the cRaf/Erk axis.

Materials and methods

Test substance (PLAG) synthesis and production

PLAG was manufactured and provided by the New Drug Production Headquarters, a Good Manufacturing Practice facility of Enzychem Lifesciences Corporation (Jecheon-si, South Korea), and was stored according to information provided by the manufacturer.

Cell culture

LLC1 cells were obtained from American Type Culture Collection (ATCC, MD, USA). Cells were grown in Dulbecco's modified Eagle medium (WelGENE, Seoul, Korea) containing 10% fetal bovine serum (RMBio, Missoula, MO, USA) and 1% antibiotics (100 mg/L streptomycin, 100 U/mL penicillin) at 37°C in a 5% CO_2 atmosphere.

Immunofluorescence staining

LLC1 cells were seeded on a glass coverslip in a 12-well plate and incubated until they reached 60% confluence. The cultures were then treated with PLAG and adenosine at 37°C in a 5% CO_2 atmosphere. The cells were then fixed with 3.7% formaldehyde for 20 min and permeabilized with 0.2% Triton X-100. To stain for specific proteins, the cells were fixed with 3.7% formaldehyde for 20 min, washed twice with phosphate-buffered saline (PBS) with Tween 20 (PBST), and incubated with specific antibodies overnight at 4°C. The cells were then washed twice with PBST and incubated with secondary antibodies. Fluorescence was detected by confocal microscopy (Carl Zeiss, Thornwood, NY, USA). The amount of fluorescence was quantified using ImageJ software.

Analysis of protein assemblies by immunoprecipitation

LLC1 cells were treated with PLAG and stimulated with adenosine for various times at 37°C in a 5% CO_2 atmosphere. The cells were then lysed in ice-cold immunoprecipitation lysis buffer (25 mM Tris-HCl, pH 7.4, 150 mM NaCl, 1% NP-40, 1 mM EDTA, 5% glycerol). The extracted proteins were incubated with Surebeads Protein G-specific antibody-bound magnetic beads (Bio-Rad, CA, USA). The beads were then washed with PBST, and the target proteins were eluted in 1 × sample buffer and analyzed by western blotting.

Analysis of protein degradation by ubiquitination assay

LLC1 cells were treated with PLAG and stimulated with adenosine for various times after pre-treatment with 10 μM MG132 for 2 hours at 37°C in a 5% CO_2 atmosphere. The cells were then lysed using ice-cold immunoprecipitation lysis buffer. The extracted proteins were incubated with Surebeads Protein G-specific antibody-bound magnetic beads (Bio-Rad), and the beads were then washed with PBST. Ubiquitinated A2BR was eluted using a 1 × non-reducing sample buffer and analyzed by western blotting.

Gene silencing by small interfering RNA (siRNA) and small hairpin RNA (shRNA)

siRNA was purchased from Thermo Fisher Scientific (Waltham, MA, USA), and the shRNA plasmid was purchased from Origene Technologies (Rockville, MD, USA). For transient transfection, cells were washed twice with PBS. The target RNA was resuspended in Opti-MEM (Thermo Fisher Scientific) containing Lipofectamine 2000 (Thermo Fisher Scientific). The target RNA mixtures were placed in a cell plate for transfection. After transfection, the cells were incubated for 72 hours for target protein silencing. Then, silenced cells were selected by treatment with 10 μg/mL puromycin for 4 days, and shRNA-transfected cells were collected.

Lysosomal activity analysis

LLC1 cells were seeded in black 96-well plates, and intracellular lysosomal activity was detected using LysoSensor (Invitrogen, Carlsbad, CA, USA). Lysosomal fluorescence was quantitatively measured with a Varioskan LUX

device (Thermo Fisher Scientific). The cells were then treated with PLAG, and LysoTracker was added using an injector. After the test dose of adenosine was administered, lysosomal fluorescence was measured at 5-min intervals. The experiment was performed at 37°C in a 5% CO_2 atmosphere

Tumor implantation (syngeneic implantation)

Five-week-old male C57BL/6J mice were obtained from Daehan Bio-Link (Yong-in, South Korea) and housed in sterile filter-topped cages. The animals (n=6 for each treatment group) were anesthetized using isoflurane and placed in the right lateral decubitus position. A total of 1×10^5 LLC1 cells in a solution containing 50 µL of culture medium and 50 µL of Matrigel (BD Biosciences, NJ, USA) were subcutaneously injected into the right-side thigh using a 29-G needle attached to a 0.5-mL insulin syringe (Becton Dickinson, NJ, USA). The mice were then allowed to rest on a heating pad until they fully recovered. Starting 3 days after cell implantation, PLAG was orally administered daily (n=6 mice per group). The positive control group (n=6 mice) was not treated. The tumor burden was calculated every 3 days after implantation. Tumor volume was approximated by a simplified ellipsoidal formula: (short axis) x (short axis) x (long axis)/2. Mice were euthanized when the longest axis of the tumor reached 2.2 cm. The animals were sacrificed 4 weeks after implantation and perfused with PBS. The tumors were extracted and fixed with 10% formaldehyde. Immunohistochemical (IHC) staining was performed on tissue sections to examine tissue morphology. All animal experiments were approved by the Institutional Animal Care and Use Committee of Korea Research Institute of Bioscience & Biotechnology (approval number: KRIBB-AEC-20130).

TXNIP-KO mice study

TXNIP-KO mice were donated by Dr. In-Pyo Choi at the Immunotherapy Convergence Research Center, Korea Research Institute of Bioscience and Biotechnology. Implantation and analysis of LLC1 cells were performed as described above .

Overall survival analysis

Kaplan–Meier survival curves were plotted for the 60-day period after cancer cell implantation. Treatments were performed until the final observation week except in cases of death or moribundity.

Immunohistochemistry staining (IHC)

Tumors were fixed in 10% formaldehyde, embedded in paraffin, and sectioned into 5-µm slices. The sections were treated with 3% H_2O_2 for 10 min to block endogenous peroxidase activity and then blocked with bovine serum albumin. Then, the sections were washed with Tris-buffered saline with Tween and incubated with specific antibodies overnight at 4°C. Negative controls were incubated with normal serum IgG for the species from which the primary antibody was obtained. The 3,3′-diaminobenzidine-stained area was analyzed using ImageJ software.

Statistics

The data were analyzed using Prism 9 (GraphPad Software, La Jolla, CA, USA). A value of $p<0.05$ was considered significant.

Results

PLAG induces anti-tumor effects and improves survival through rapid A2BR degradation

The tumor burden was observed in syngeneic LLC1 cell-implanted mice, and the anti-tumor effect of PLAG was investigated according to the experimental schedule (Figure 1A). The tumor size increased markedly 2 weeks after implantation, and approximately 5 g of tumor tissue was observed 27 days after drug delivery. However, tumor growth was clearly delayed by PLAG treatment (Figure 1B, C). The tumor weight was decreased by 65% in 50 mg/kg PLAG-treated mice and by 86% in 100 mg/kg PLAG-treated mice (Figure 1D). Over 60 days, five of six mice died in the positive control group, and five of six mice survived in the group treated with 50 mg/kg PLAG (Figure 1E).

A2BR expression and cRaf/Erk phosphorylation were observed in tumor tissue. However, reduced A2BR expression and dephosphorylation of the cRaf/Erk axis were observed in mice treated with PLAG. High expression levels of TXNIP, which are closely related to biological activities, such as the promotion of A2BR degradation and the reduction of cRaf/Erk axis activity, were observed in PLAG-treated mice (Figure 1F–H).

PLAG promotes A2BR degradation by activating ubiquitination

The early termination of cRaf/Erk axis signaling and its effect on cell proliferation after A2BR degradation in PLAG-treated cells were verified using adenosine-treated LLC1 cells. Western blotting of adenosine-treated cells showed that cRaf/Erk signaling activity occurred for 6 hours in the presence of A2BRs, whereas A2BR degradation and cRaf/Erk inactivation were observed within 3 hours in PLAG co-treated cells (Figure 2A). Ubiquitination, which is a major cause of A2BR degradation, was observed within 3 hours in PLAG co-treated cells. Furthermore, PLAG treatment increased A2BR ubiquitination and lysosome activity (Figure 2B, D). Complexes containing A2BRs, β-arrestin-2, and phosphatase 2A (PP2A) were detected in adenosine-treated cells. When β-arrestin-2 and PP2A assemble, Rab4 is recruited, and this combination promotes receptor endocytosis and intracellular trafficking and facilitates the return of the receptor to the membrane. By contrast, in PLAG co-treated cells, A2BR bound to TXNIP, followed by binding to β-arrestin-1 and -2 and the E3 ligase neural precursor cell-expressed developmentally downregulated protein 4 (NEDD4) (Figure 2C, E, F and Supplementary Figure 2). The NEDD4–A2BR complex underwent ubiquitination and receptor degradation.

PLAG induces TXNIP expression and membrane localization

The TXNIP expression level in PLAG-treated cells was examined by western blotting, and TXNIP localization was examined by confocal microscopy. TXNIP showed increased expression in PLAG-treated cells and was localized to plasma membranes, suggesting that PLAG plays a major role in the rapid internalization and degradation of A2BR receptors (Figure 3).

Anti-tumor effects of PLAG during tumor progression

The anti-tumor effects of PLAG in LLC1 cell-implanted mice, including tumor size and A2BR-mediated signal modulation, were analyzed weekly. The size and weight of tumors did not increase in PLAG-treated mice during tumor development (Figure 4A). In particular, TXNIP expression decreased with tumor growth in mice but was maintained in PLAG-treated mice. cRaf/Erk phosphorylation, which is considered a major signal for tumor growth, was observed in untreated mice but not in PLAG-treated mice (Figure 4C–F). These results suggest that the A2BR/cRaf/Erk axis is directly

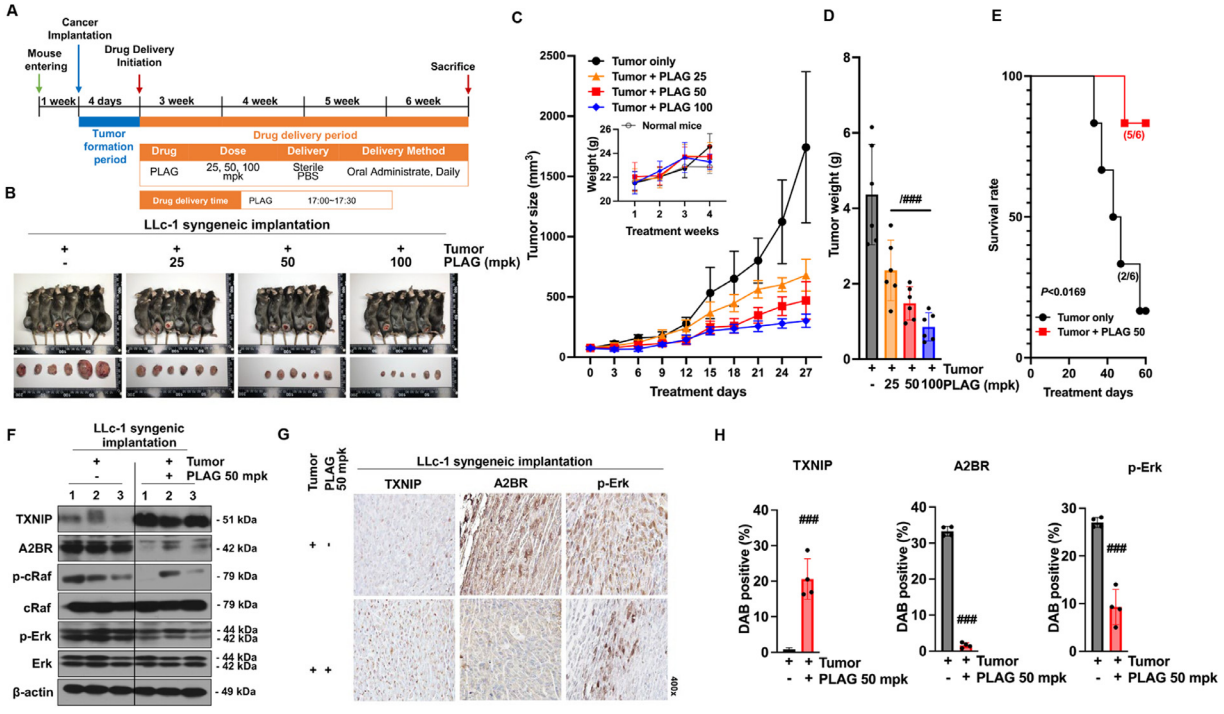

Figure 1. Analysis of the effectiveness of PLAG on tumor development. **A.** Experimental design used to assess the effects of PLAG in an LLC1-implanted syngeneic mouse model. **B.** Tumor size reduction in PLAG-treated mice. **C.** The increase in tumor size in each group was estimated at 3-day intervals. **D.** The reduction in tumor weight was calculated in mice treated with PLAG for 4 weeks. **E.** Analysis of survival rates for PLAG-treated mice (survival/test mice). **F.** Protein expression and phosphorylation in tumor-induced tissues were analyzed using western blotting. **G, H.** Proteins associated with tumor progression were analyzed using immunohistochemical (IHC) staining. Compared to normal mice: $^{***}p<0.001$; Compared to the tumor only: $\#p<0.033$, $\#\#\#p<0.001$ (each experiment n=6, n=4 for IHC analysis). N.S, Not significant. Mean±SD.

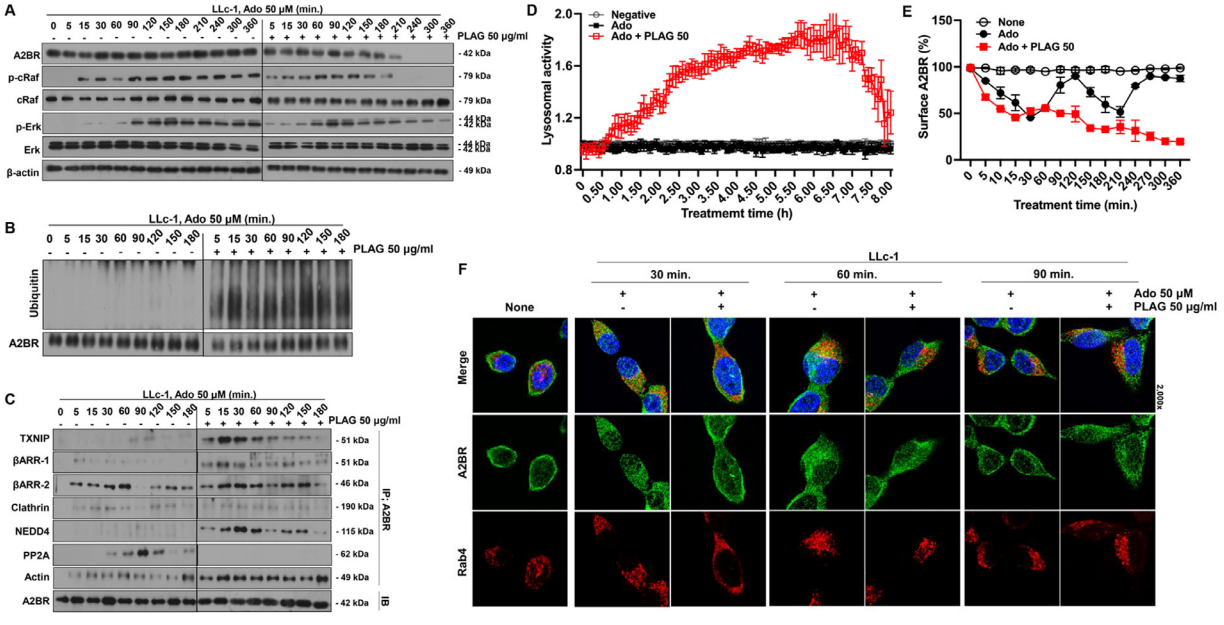

Figure 2. PLAG promotes degradation of A2BR through receptor ubiquitination. **A.** Alterations of A2BRs and signaling molecules in cells co-treated with adenosine and PLAG were tracked over time. **B.** Ubiquitination of A2BRs in cells co-treated with adenosine and PLAG. **C.** Changes in proteins associated with A2BR degradation in cells treated with adenosine alone or co-treated with PLAG. **D.** Lysosomal activity in PLAG-treated cells. **E.** Analysis of intracellular A2BR trafficking in cells co-treated with adenosine and PLAG. **F.** Recycling and co-localization of Rab4 and A2BRs in PLAG-treated cells (blue, nucleus; green, A2BR; red, Rab4).

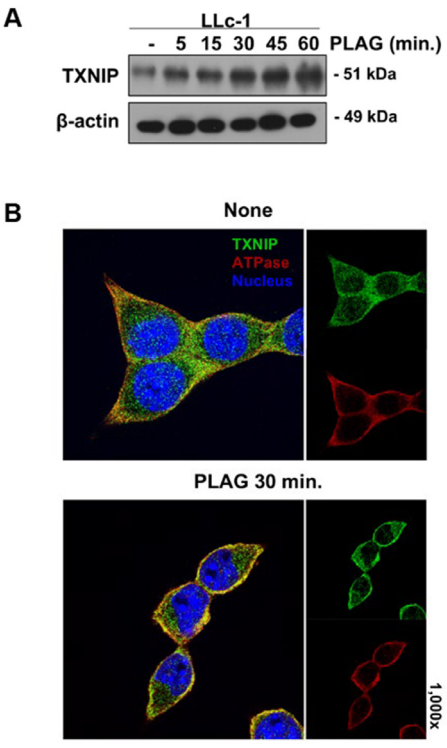

Figure 3. PLAG promoted TXNIP expression and re-localization to the membrane. **A.** TXNIP expression in PLAG-treated LLC1 cells. **B.** TXNIP was located in the cell membranes of cells treated with PLAG.

linked to tumor overgrowth. Ubiquitination of A2BRs (i.e., degradation) was continuously observed in PLAG-treated mice and is suggested to play an essential role in reducing tumor progression.

PLAG-mediated activities, such as A2BR degradation and anti-tumor signaling, are not observed in TXNIP-silenced cells

The effectiveness of PLAG in TNXIP-silenced LLC1 cells was analyzed to verify the role of PLAG in inhibiting TXNIP-dependent tumor growth and the early termination of cRaf/Erk axis signaling by A2BR degradation. LLC1 cell growth was completely attenuated after adenosine treatment in PLAG co-treated cells, and this effect was absent in TXNIP-silenced cells (Supplementary Figure 4). Additionally, the A2BR degradation and cRaf/Erk dephosphorylation observed in PLAG-treated cells were not observed in TXNIP-silenced cells (Figure 5A). The ubiquitination and lysosomal activity involved in A2BR degradation in PLAG-treated cells were also absent in TXNIP-silenced cells (Figure 5B–D). TXNIP recruits A2BR complex proteins, such as β-arrestin-1/NEDD4, to degrade internalized receptors, but A2BRs bound to β-arrestin-2/PP2A in TXNIP-silenced cells return to the membrane, resulting in receptor recycling (Figure 5E–G).

The anti-tumor effects of PLAG are dependent on the regulation of TXNIP expression in tumors

The anticancer effect of PLAG was investigated in TXNIP-silenced cell-implanted mice. Compared with that in wild-type (WT) cell-implanted mice, a greater than 70% decrease in the inhibition of tumor progression was observed when PLAG was administered to TXNIP-silenced cell-implanted mice (Figure 6A). The 60-day survival rate was 100% in PLAG-treated mice implanted with WT cells. However, five of six mice implanted with TXNIP-silenced cells died, with no PLAG-mediated increase in survival rate

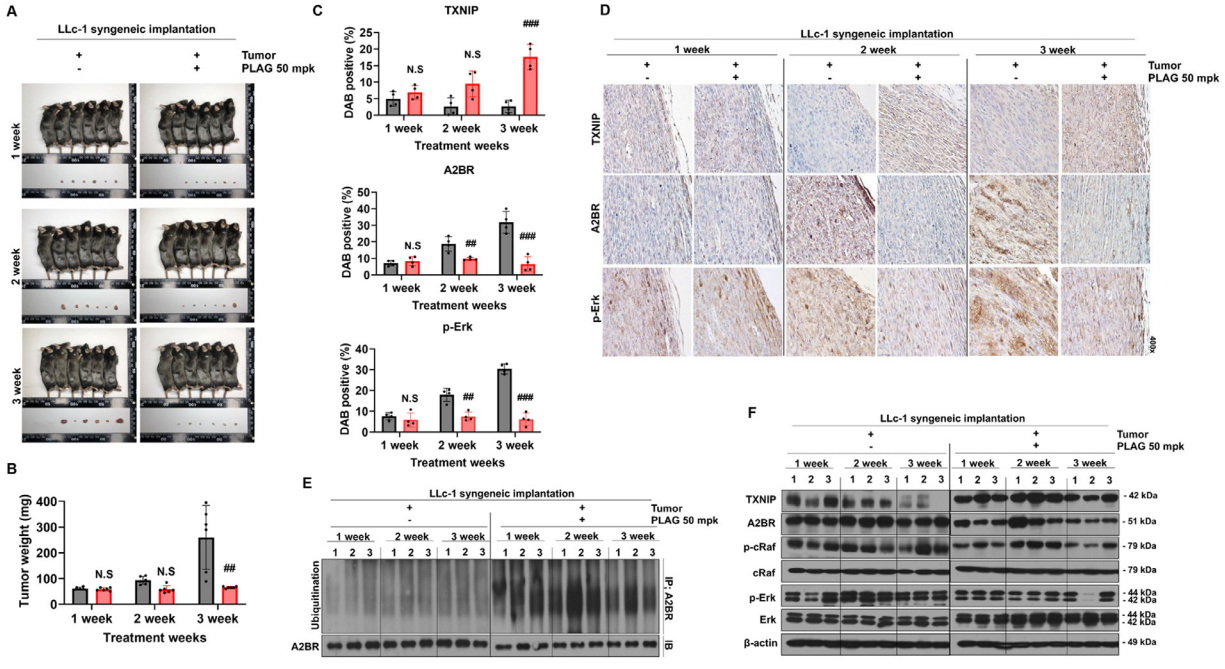

Figure 4. Weekly analysis of antitumor effects of PLAG and TXNIP expression in tumor-implanted mice. **A, B.** The anti-tumor efficacy of PLAG was evaluated weekly for 3 weeks through analysis of tumor growth in LLC1 cell-implanted mice. **C, D.** The protein expression profiles of A2BR, TXNIP, and p-Erk, were analyzed weekly using IHC staining of tumors. **E.** Ubiquitination of A2BRs was evaluated weekly in tumors. **F.** Modification of A2BRs and signal-related proteins in tumors was analyzed by western blotting for 3 weeks. Compared to the tumor only: #$p<0.033$, ###$p<0.001$ (each experiment n=6, n=4 for IHC analysis). N.S, not significant. Mean±SD.

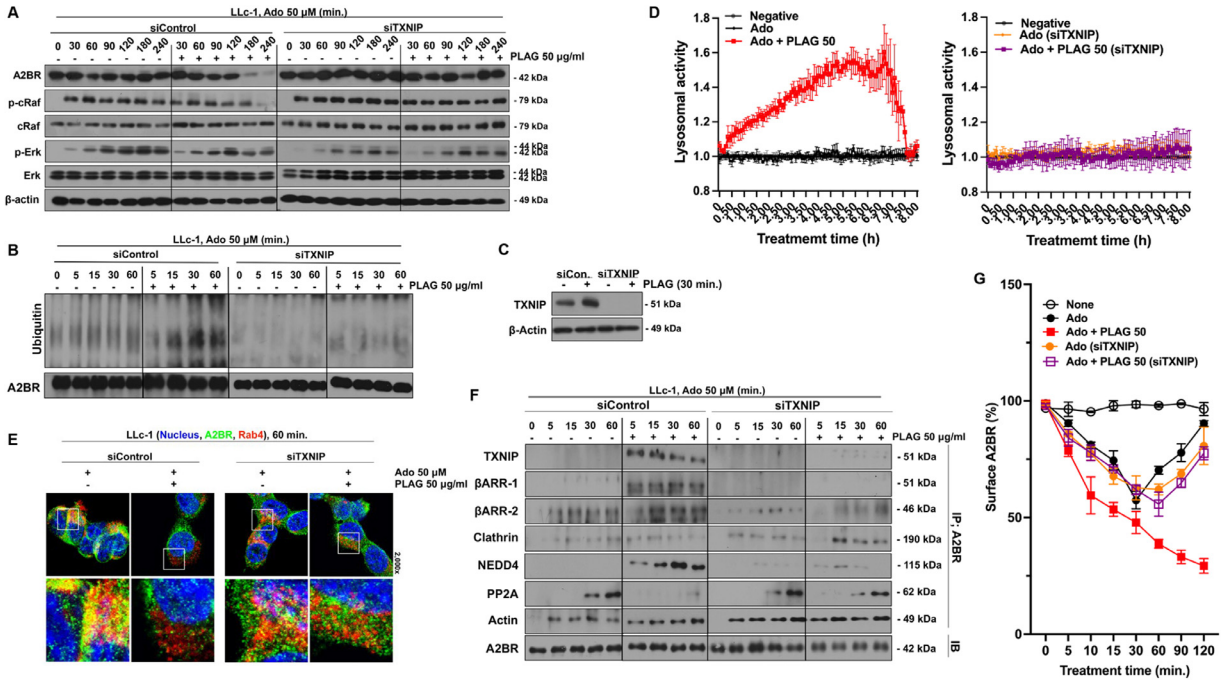

Figure 5. Accelerated A2BR degradation by ubiquitin activation depends on TXNIP expression in PLAG-treated cells. **A.** Acceleration of A2BR degradation and decreased cRaf/Erk phosphorylation after PLAG treatment were not detected in TXNIP-silenced cells. **B.** Increased ubiquitination of A2BRs with PLAG treatment was not observed in TXNIP-silenced cells. **C.** Knockdown of TXNIP protein was confirmed in TXNIP-silenced cells. **D.** PLAG treatment did not induce lysosomal activity in TXNIP-silenced cells. **E.** Co-localization of A2BRs and Rab4 was not observed in cells co-treated with adenosine and PLAG, but this effect was observed in TXNIP-silenced cells. **F.** A2BR-related proteins that regulate intracellular trafficking were analyzed in TXNIP-silenced cells. **G.** Internalized A2BRs in adenosine-treated cells returned to the cell membrane (recycling), but internalized A2BRs were not returned to the cell membrane in cells co-treated with adenosine and PLAG. This effect of PLAG was not observed in TXNIP-silenced cells.

(Figure 6B). TXNIP is a tumor suppressor protein [37,38], and TXNIP-silenced tumors may exhibit an aggressive phenotype. Additionally, PLAG did not reduce tumor size in TXNIP-silenced cell-implanted mice (Figure 6C). Modification of intracellular signaling-related proteins, such as A2BRs, and reduction of cRaf/Erk activity by PLAG treatment were not observed in TXNIP-silenced tumor-bearing mice (Figure 6D). Tumor tissue analysis of TXNIP-silenced tumor-bearing mice showed that they did not exhibit A2BR degradation or reduced cRaf/Erk phosphorylation (Figure 6E). PLAG had anticancer effects in TXNIP-KO mice implanted with WT tumors, whereas PLAG did not produce these effects in TXNIP-KO mice implanted with TXNIP-silenced tumors (Supplementary Figure 6). Therefore, PLAG-mediated induction of TXNIP in tumor tissue plays a pivotal role in the anticancer effects of PLAG.

Discussion

Recent reports have shown that adenosine plays an important role in the TME, resulting in tumor growth. In particular, activation of A2BRs by adenosine induces excessive tumor formation and creates a tumor-promoting microenvironment in which tumors can grow excessively by activating multiple signaling pathways, such as the MAPK pathway and Akt axis. Thus, targeting approaches to regulate A2BR activity is an important therapeutic area for anticancer research.

This study demonstrates the effect of inhibiting tumor overgrowth by inducing A2BR degradation through PLAG treatment. In the LLC1 cell-implanted mouse model, PLAG reduced tumor size and significantly increased the survival rate (Figure 1). Specifically, PLAG effectively reduced the A2BR level and the activity of the cRaf/Erk receptor-mediated signaling pathway, which is involved in tumor progression (Figure 1F–H and Figure 2A). PLAG has a unique mechanism of action through which receptor-mediated signaling is terminated by rapid receptor degradation after initial activation, unlike conventional antagonists that inhibit receptor activity (Figure 2C–G and Supplementary Figure 3). Increased A2BR/cRaf/Erk axis activation results in tumor overgrowth. However, PLAG reduced cRaf/Erk phosphorylation via A2BR degradation. As a result, tumor overgrowth was suppressed, and proliferation-related signaling pathways were terminated (Figure 4 and Supplementary Figure 1). As shown in Figures 2B, D, and 4E, A2BR ubiquitination and lysosomal activity were only increased in PLAG-treated cells.

Initially, PLAG induced the expression of TXNIP, a type of α-arrestin (Figure 3). The increased TXNIP protein level in PLAG-treated cells caused recruitment and co-binding of the NEDD4 and β-arrestin-1 complex to A2BRs (Figure 2C). According to recent reports, receptor binding to β-arrestin-1, but not β-arrestin-2, is induced by the NEDD4 complex [39–42]. Therefore, receptor binding of the $\boldsymbol{\alpha}$-arrestin family, which contains PPxY motifs, causes lysosomal degradation [43,44]. A2BR degradation by PLAG-induced TXNIP was confirmed in experiments using TXNIP-silenced cells (Figure 5). Failure of PLAG to inhibit tumor growth was observed in mice implanted with TXNIP-silenced tumor cells (Figure 6 and Supplementary Figure 4).

Another result of the ability of PLAG to promote receptor complex formation via TXNIP expression is the degradation of GPCRs, including PAR2, and epidermal growth factor receptor (EGFR) [35,36]. Internalized receptor degradation may ultimately interfere with the intracellular signaling of ligand-binding receptors.

Endosome signaling during intracellular GPCR trafficking is considered an essential pathway in cancer development and is of significant interest for drug discovery [45–48]. To date, the abilities of many GPCR signal-

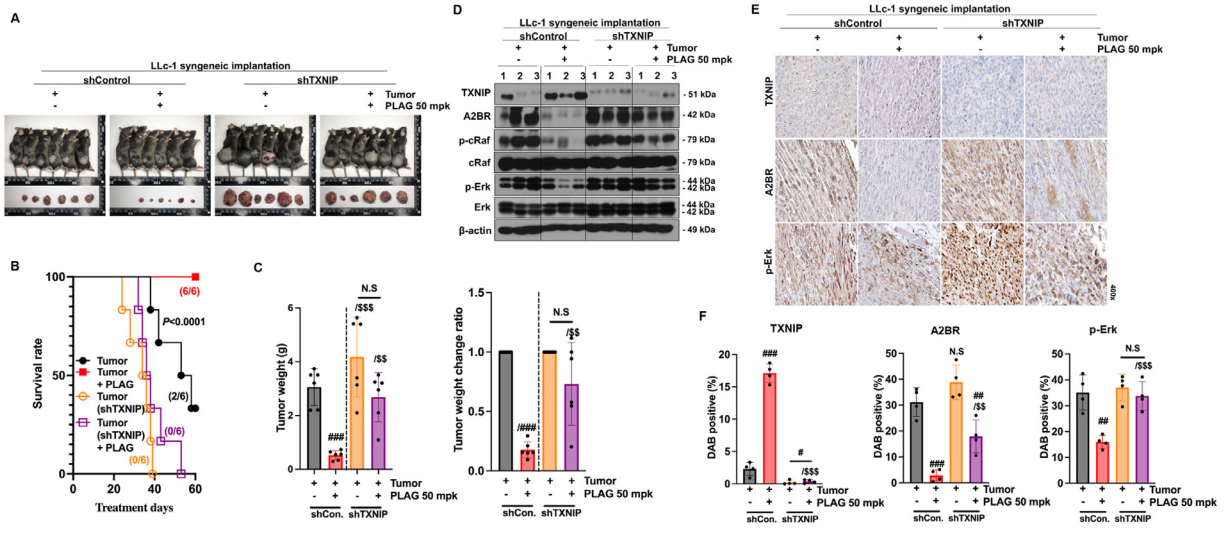

Figure 6. The effects of PLAG on tumor suppression are not observed in TXNIP-silenced cell-implanted mice. **A, B.** The inhibition of tumor growth and increase in survival rate resulting from PLAG treatment were not observed in TXNIP-silenced cell-implanted mice. **C.** In TXNIP-silenced cell-implanted mice, tumor weight did not decrease with PLAG treatment. **D–F.** In TXNIP-silenced cell-implanted mice, the degradation of A2BRs and reduction of cRaf/Erk phosphorylation induced by PLAG treatment were not observed. Compared to normal mice: $^{***}p<0.001$; Compared to the tumor only: $\#p<0.033$, $\#\#\#p<0.001$; Compared to PLAG treatment of TXNIP-WT cells: $\$p<0.033$, $\$\$\$p<0.001$ (each experiment n=6). N.S, not significant. Mean±SD.

modulating drugs to competitively inhibit ligand–receptor binding have been studied [49,50]. The use of receptor antagonist strategies can cause substantial side effects due to the inhibition of critical signaling pathways essential for host defense. However, PLAG can attenuate excessive and continuous signaling through the degradation of activated receptors rather than the inactivation of receptors. This unique mechanism of action involves receptor degradation via the induction of TXNIP expression. PLAG has potential as a highly effective anti-tumor agent that can sufficiently replace antagonists, which can cause side effects and excessive secondary pathway activity by blocking signaling pathways through simple inhibition.

Funding

This work was supported by the KRIBB Research Initiative Program (grant number KGM5252221) and grants from Enzychem Lifesciences (grant numbers IGM0382211 and IGM0402111).

Author contribution

Guen Tae Kim: Writing – Original draft, Methodology, Validation, Investigation, Formal analysis, Data curation Eun Young Kim: Investigation, Formal analysis Su-Hyun Shin: Investigation Hyowon Lee: Investigation Se Hee Lee: Investigation Ki-Young Sohn: Funding acquisition Jae Wha Kim: Project administration, Supervision, Conceptualization, Writing – Review & editing.

Declaration of Competing Interest

The authors declare no potential conflicts of interest.

Acknowledgments

Corresponding author J.W.K. declares that the research was conducted in the absence of any commercial or financial relationships that could be constructed as a potential conflict of interest. The authors thank Dr. Larry Kwak and Dr. Jeffrey Crawford for guidance and insightful discussions.

References

[1] Di Virgilio F, Adinolfi E. Extracellular purines, purinergic receptors and tumor growth. *Oncogene* 2017;**36**:293–303.

[2] Allard B, Allard D, Buisseret L, Stagg J. The adenosine pathway in immuno-oncology. *Nat Rev Clin Oncol* 2020;**17**:611–29.

[3] Vijayan D, Young A, Teng MWL, Smyth MJ. Targeting immunosuppressive adenosine in cancer. *Nat Rev Cancer* 2017;**17**:709–24.

[4] Mittal D, Sinha D, Barkauskas D, Young A, Kalimutho M, Stannard K, Caramia F, Haibe-Kains B, Stagg J, Khanna KK, Loi S, Smyth MJ. Adenosine 2B receptor expression on cancer cells promotes metastasis. *Cancer Res* 2016;**76**:4372–82.

[5] Lan J, Lu H, Samanta D, Salman S, Lu Y, Semenza GL. Hypoxia-inducible factor 1-dependent expression of adenosine receptor 2B promotes breast cancer stem cell enrichment. *Proc Natl Acad Sci U S A,* 2018;**115**:E9640–8.

[6] Vecchio EA, White PJ, May LT. The adenosine A2B G protein-coupled receptor: recent advances and therapeutic implications. *Pharmacol Ther* 2019;**198**:20–33.

[7] Chen S, Akdemir I, Fan J, Linden J, Zhang B, Cekic C. The expression of adenosine A2B receptor on antigen-presenting cells suppresses CD8+ T-cell responses and promotes tumor growth. *Cancer Immunol Res* 2020;**8**:1064–74.

[8] C. Giacomelli, S. Daniele, C. Romei, L. Tavanti, T. Neri, I. Piano, A. Celi, C. Martini, M.L. Trincavelli, The A2B Adenosine Receptor Modulates the Epithelial– Mesenchymal Transition through the Balance of cAMP/PKA and MAPK/ERK Pathway Activation in Human Epithelial Lung Cells, 9 (2018).

[9] Allard B, Beavis PA, Darcy PK, Stagg J. Immunosuppressive activities of adenosine in cancer. *Curr Opin Pharmacol* 2016;**29**:7–16.

[10] Wei Q, Costanzi S, Balasubramanian R, Gao Z-G, Jacobson KA. A2B adenosine receptor blockade inhibits growth of prostate cancer cells. *Purinergic Signall* 2013;**9**:271–80.

[11] Walters MJ, Piovesan D, Tan J, DiRenzo D, Yin F, Miles D, Leleti MR, Park T, Soriano F, Sharif E. *Combining adenosine receptor inhibition with AB928 and chemotherapy results in greater immune activation and tumor control.* AACR; 2018.

[12] Cekic C, Sag D, Li Y, Theodorescu D, Strieter RM, Linden J. Adenosine A2B receptor blockade slows growth of bladder and breast tumors. *J Immunol (Baltimore, Md.: 1950)* 2012;**188**:198–205.

[13] Peterson YK, Luttrell LM. The diverse roles of arrestin scaffolds in g protein-coupled receptor signaling. *Pharmacol Rev* 2017;**69**:256–97.

[14] Lee MH, Appleton KM, Strungs EG, Kwon JY, Morinelli TA, Peterson YK, Laporte SA, Luttrell LM. The conformational signature of beta-arrestin2 predicts its trafficking and signalling functions. *Nature* 2016;**531**:665–8.

[15] Baidya M, Kumari P, Dwivedi-Agnihotri H, Pandey S, Sokrat B, Sposini S, Chaturvedi M, Srivastava A, Roy D, Hanyaloglu AC, Bouvier M, Shukla AK. Genetically encoded intrabody sensors report the interaction and trafficking of beta-arrestin 1 upon activation of G-protein-coupled receptors. *J Biol Chem* 2020;**295**:10153–67.

[16] Hilger D, Masureel M, Kobilka BK. Structure and dynamics of GPCR signaling complexes. *Nat Struct Mol Biol* 2018;**25**:4–12.

[17] Pavlos NJ, Friedman PA. GPCR signaling and trafficking: the long and short of it. *Trends Endocrinol Metab* 2017;**28**:213–26.

[18] Rosenbaum DM, Rasmussen SG, Kobilka BK. The structure and function of G-protein-coupled receptors. *Nature* 2009;**459**:356–63.

[19] Zielinska KA, Katanaev VL. Information theory: new look at oncogenic signaling pathways. *Trends Cell Biol* 2019;**29**:862–75.

[20] Ranjan R, Gupta P, Shukla AK. GPCR Signaling: beta-arrestins Kiss and Remember. *Curr Biol* 2016;**26**:R285–8.

[21] Eichel K, Jullie D, von Zastrow M. beta-Arrestin drives MAP kinase signalling from clathrin-coated structures after GPCR dissociation. *Nat Cell Biol* 2016;**18**:303–10.

[22] Gurevich VV, Gurevich EV. Arrestins: Critical Players in Trafficking of Many GPCRs. *Prog Mol Biol Transl Sci* 2015;**132**:1–14.

[23] Shukla AK, Kim J, Ahn S, Xiao K, Shenoy SK, Liedtke W, Lefkowitz RJ. Arresting a transient receptor potential (TRP) channel: beta-arrestin 1 mediates ubiquitination and functional down-regulation of TRPV4. *J Biol Chem* 2010;**285**:30115–25.

[24] Srivastava A, Gupta B, Gupta C, Shukla AK. Emerging functional divergence of beta-arrestin isoforms in GPCR function. *Trends Endocrinol Metab* 2015;**26**:628–42.

[25] Pandey S, Mahato PK, Bhattacharyya S. Metabotropic glutamate receptor 1 recycles to the cell surface in protein phosphatase 2A-dependent manner in non-neuronal and neuronal cell lines. *J Neurochem* 2014;**131**: 602–614.

[26] Waldhart AN, Dykstra H, Peck AS, Boguslawski EA, Madaj ZB, Wen J, Veldkamp K, Hollowell M, Zheng B, Cantley LC, McGraw TE, Wu N. Phosphorylation of TXNIP by AKT mediates acute influx of glucose in response to insulin. *Cell Rep* 2017;**19**:2005–13.

[27] Wu N, Zheng B, Shaywitz A, Dagon Y, Tower C, Bellinger G, Shen C-H, Wen J, Asara J. Timothy, Barbara, Lewis, AMPK-dependent degradation of TXNIP upon energy stress leads to enhanced glucose uptake via GLUT1. *Molecular Cell* 2013;**49**:1167–75.

[28] Han SO, Kommaddi RP, Shenoy SK. Distinct roles for beta-arrestin2 and arrestin-domain-containing proteins in beta2 adrenergic receptor trafficking. *EMBO Rep* 2013;**14**:164–71.

[29] Lee S, Park S, Lee H, Han S, Song JM, Han D, Suh YH. Nedd4 E3 ligase and beta-arrestins regulate ubiquitination, trafficking, and stability of the mGlu7 receptor. *Elife* 2019;**8**.

[30] J.G. N Dores MR, Lin H, Mendez F, Trejo J. The alpha-arrestin ARRDC3 mediates ALIX ubiquitination and G protein-coupled receptor lysosomal sorting. *Mol Biol Cell* 2015;**26**:4660–73.

[31] Lee HR, Shin SH, Kim JH, Sohn KY, Yoon SY, Kim JW. 1-Palmitoyl-2-Linoleoyl-3-Acetyl-rac-Glycerol (PLAG) Rapidly Resolves LPS-Induced Acute Lung Injury Through the Effective Control of Neutrophil Recruitment. *Front Immunol* 2019;**10**:2177.

[32] Lee H-R, Shin S-H, Yoo N, Yoon SY, Kim JH, Nah S-S, Kim M-H, Sohn K-Y, Kim H-J, Chong S, Han Y-H, Kim JW. Prevention of LPS-induced lung inflammation by PLAG administration via blocking of IL-6-STAT3-MIP-2 pathway. *J Immnunol* 2016;**196** 50.52-50.52.

[33] Lee H-R, Yoo N, Kim J, Sohn K-Y, Kim H-J, Kim M-H, Han M, Yoon S, Kim J. The therapeutic effect of PLAG against oral mucositis in hamster and mouse model. *Front Oncol* 2016;**6**:209.

[34] Shin SH, Jeong J, Kim JH, Sohn KY, Yoon SY, Kim JW. 1-Palmitoyl-2-Linoleoyl-3-Acetyl-rac-Glycerol (PLAG) mitigates monosodium Urate (MSU)-Induced Acute Gouty Inflammation in BALB/c Mice. *Front Immunol* 2020;**11**:710.

[35] Kim GT, Hahn KW, Yoon SY, Sohn KY, Kim JW. PLAG exerts anti-metastatic effects by interfering with neutrophil elastase/PAR2/EGFR signaling in A549 lung cancer orthotopic model. *Cancers (Basel)* 2020:12.

[36] Yang KH, Kim GT, Choi S, Yoon SY, Kim JW. 1–Palmitoyl–2–linoleoyl–3–acetyl–rac–glycerol ameliorates EGF–induced MMP–9 expression by promoting receptor desensitization in MDA–MB–231 cells. *Oncol Rep* 2020;**44**:241–51.

[37] Chen Y, Ning J, Cao W, Wang S, Du T, Jiang J, Feng X, Zhang B. Research progress of TXNIP as a tumor suppressor gene participating in the metabolic reprogramming and oxidative stress of cancer cells in various cancers. *Front Oncol* 2020;**10**.

[38] Xie M, Xie R, Xie S, Wu Y, Wang W, Li X, Xu Y, Liu B, Zhou Y, Wang T, Gao L, Pan T. Thioredoxin interacting protein (TXNIP) acts as a tumor suppressor in human prostate cancer. *Cell Biol Int* 2020;**44**:2094–106.

[39] Shea FF, Rowell JL, Li Y, Chang TH, Alvarez CE. Mammalian alpha arrestins link activated seven transmembrane receptors to Nedd4 family e3 ubiquitin ligases and interact with beta arrestins. *PLoS One* 2012;**7**:e50557.

[40] Grimsey NJ, Narala R, Rada CC, Mehta S, Stephens BS, Kufareva I, Lapek J, Gonzalez DJ, Handel TM, Zhang J, Trejo J. A tyrosine switch on NEDD4-2 E3 ligase transmits GPCR inflammatory signaling. *Cell Rep* 2018;**24** 3312-3323 e3315.

[41] Dores MR, Trejo J. Endo-lysosomal sorting of G-protein-coupled receptors by ubiquitin: diverse pathways for G-protein-coupled receptor destruction and beyond. *Traffic* 2019;**20**:101–9.

[42] Shao G, Wang R, Sun A, Wei J, Peng K, Dai Q, Yang W, Lin Q. The E3 ubiquitin ligase NEDD4 mediates cell migration signaling of EGFR in lung cancer cells. *Mol Cancer* 2018;**17**:24.

[43] Arakaki AKS, Pan WA, Lin H, Trejo J. The alpha-arrestin ARRDC3 suppresses breast carcinoma invasion by regulating G protein-coupled receptor lysosomal sorting and signaling. *J Biol Chem* 2018;**293**:3350–62.

[44] Tian X, Irannejad R, Bowman SL, Du Y, Puthenveedu MA, von Zastrow M, Benovic JL. The alpha-Arrestin ARRDC3 Regulates the Endosomal Residence Time and Intracellular Signaling of the beta2-Adrenergic Receptor. *J Biol Chem* 2016;**291**:14510–25.

[45] Usman S, Khawer M, Rafique S, Naz Z, Saleem K. The current status of anti-GPCR drugs against different cancers. *J Pharm Anal* 2020;**10**:517–21.

[46] Insel PA, Sriram K, Wiley SZ, Wilderman A, Katakia T, McCann T, Yokouchi H, Zhang L, Corriden R, Liu D, Feigin ME, French RP, Lowy AM, Murray F. GPCRomics: GPCR Expression in Cancer Cells and Tumors Identifies New, Potential Biomarkers and Therapeutic Targets. *Front Pharmacol* 2018;**9**:431.

[47] Hauser AS, Attwood MM, Rask-Andersen M, Schioth HB, Gloriam DE. Trends in GPCR drug discovery: new agents, targets and indications. *Nat Rev Drug Discov* 2017;**16**:829–42.

[48] Hauser AS, Chavali S, Masuho I, Jahn LJ, Martemyanov KA, Gloriam DE, Babu MM. Pharmacogenomics of GPCR Drug Targets. *Cell* 2018;**172**:41–54 e19.

[49] Basith S, Cui M, Macalino SJY, Park J, Clavio NAB, Kang S, Choi S. Exploring G protein-coupled receptors (GPCRs) ligand space via cheminformatics approaches: impact on rational drug design. *Front Pharmacol* 2018;**9**:128.

[50] Congreve M, de Graaf C, Swain NA, Tate CG. Impact of GPCR structures on drug discovery. *Cell* 2020;**181**:81–91.